Environmental Science and Pollution Research (2018) 25:29017–29025
https://doi.org/10.1007/s11356-018-2909-y

RESEARCH ARTICLE

Removal mechanism of sulfamethazine and its intermediates from water by a rotating advanced oxidation contactor equipped with TiO_2–high-silica zeolite composite sheets

Shuji Fukahori[1] · Misaki Ito[2] · Taku Fujiwara[3]

Received: 21 April 2018 / Accepted: 3 August 2018 / Published online: 14 August 2018

Abstract

The removal of antibiotic sulfamethazine (SMT) and its intermediates from water was investigated using a rotating advanced oxidation contactor (RAOC) equipped with TiO_2-high-silica zeolite composite sheets. SMT was readily removed from water through adsorption onto high-silica zeolite and photocatalytic decomposition by TiO_2 inside the composite sheet. Some degradation intermediates were retained and photocatalytically decomposed inside the composite sheet. Relatively hydrophobic intermediates such as hydroxylated SMT were captured inside the sheets, whereas hydrophilic intermediates were distributed in water. This was attributed to the hydrophobic interactions in the adsorption mechanism of high-silica zeolite. The time courses of the NH_4^+, NO_3^-, and SO_4^{2-} ion concentration during the RAOC treatment of SMT were evaluated. After treatment by RAOC for 24 h, approximately 94% of nitrogen derived from the amino and sulfanilamide groups and 39% of sulfur from the sulfanilamide group were mineralized, which indicated that the mineralization behavior of SMT treated by RAOC was different from that treated by TiO_2 powder. These results strongly suggested that the dissociation of the amino group and cleavage of the sulfonamide group and subsequent dissociation of the amino group preferentially proceeded inside the composite sheets.

Keywords Rotating advanced oxidation contactor · TiO_2-zeolite composite sheets · Sulfonamide antibiotics · Intermediate products · Adsorption · Mineralization

Introduction

Pharmaceuticals and compounds derived from personal care products are often detected in the secondary effluent of wastewater treatment plants or in local aquatic systems (Lapworth et al. 2012: Kim et al. 2013: Li et al. 2013). For the sustainable use of water, safe and cost-effective methods for the removal of these compounds from wastewater are required. Water purification methods including advanced oxidation processes such as ultraviolet (UV) irradiation, ozonation, the Fenton reaction, and photocatalytic decomposition, as well as adsorption, have been applied (Fukahori et al. 2012: Prieto-Rodriguez et al. 2012: Cao et al. 2013: Gao et al. 2014: Ji et al. 2014: Kordkandi and Rasoul 2015: Lian et al. 2015: Kordkandi and Motlagh 2018). TiO_2, the representative photocatalyst, had high oxidizing power and could decompose recalcitrant organic compounds under UV irradiation. However, a few hours were needed to remove the pollutants from water (Prieto-Rodriguez et al. 2012; Fukahori et al. 2012; Cao et al. 2013; Fukahori and Fujiwara 2015). In contrast, adsorption occurs quickly compared with photocatalysis, although it stops after saturation is reached (Fukahori et al. 2011; Fukahori et al. 2013). To overcome the disadvantages of each material, photocatalysts and adsorbents have been compounded and applied for the removal of pharmaceuticals in water (Zhao et al. 2010; Yap and Lim 2012; Yap et al.

Responsible editor: Suresh Pillai

Electronic supplementary material The online version of this article (https://doi.org/10.1007/s11356-018-2909-y) contains supplementary material, which is available to authorized users.

✉ Taku Fujiwara
fujiwarat@kochi-u.ac.jp

[1] Paper Industry Innovation Center of Ehime University, Shikokuchuo, Japan

[2] Graduate School of Integrated Arts and Sciences, Kochi University, Kochi, Japan

[3] Research and Education Faculty, Natural Sciences Cluster, Agriculture Unit, Kochi University, 200 Monobe Otsu, Nankoku, Kochi 783-8502, Japan

2012). We have also synthesized TiO_2–zeolite composites for the removal of sulfonamide antibiotics in secondary effluent (Ito et al. 2014). The composites could remove sulfonamide from secondary effluent more effectively than TiO_2 alone. Furthermore, the synergistic effect between TiO_2 and adsorbent was kinetically revealed (Fukahori et al. 2011). However, microfiltration was needed for the recovery of the catalyst because of the small particle size of the powdery composites. Therefore, much research has been undertaken to immobilize functional materials onto a suitable supporting matrix for practical applications (Hegedűs et al. 2017; Rimoldi et al. 2017).

Previously, we prepared composite TiO_2–high-silica zeolite sheets using a papermaking technique and developed a novel rotating advanced oxidation contactor (RAOC) for selective removal of sulfonamide antibiotics from the urine of livestock (Fukahori et al. 2015). The prepared composite sheet was easy to handle and could be attached to a rotating contactor. With respect to the application of photocatalyst, Dionysiou et al. suggested rotating disk photocatalytic reactor and investigated the relationship between the operation parameters such as angular velocity of rotating disk and UV intensity (Dionysiou et al. 2000). One of the advantages of rotating disk reactor was that photocatalytic decomposition occurred in a thin liquid film formed at the disk surface; therefore, light attenuation by water might be mitigated. Zhang et al. developed disk and drum type photocatalytic rotating reactor and studied the effects of reactor shape, rotating speed, and UV intensity (Zhang et al. 2006). They found the photocatalytic decomposition rate was low at low rotation speed because the water film was too thin to provide enough target compound to disk surface; therefore, the retention of the target compound at disk surface is one of the essential steps. Our RAOC reactor could photocatalytically decompose sulfamethazine (SMT) in synthetic urine even though high amounts of co-existing materials such as urea and inorganic ions were present because high-silica zeolite inside the sheet selectively adsorb SMT. However, the removal mechanism of SMT by RAOC reactor was not clear.

In the present study, the mechanism for the removal of SMT and its degradation intermediates through photocatalysis was clarified by investigating the formation and localization behavior of the compounds in the RAOC reactor. In addition, the mineralization of SMT was quantitatively evaluated through the measurement of the organic carbon content and the NH_4^+, NO_3^-, and SO_4^{2-} ion concentrations in treated water.

Materials and methods

Materials

High-silica Y-type zeolite (HSZ-385; surface area, 600 m^2/g; $SiO_2/Al_2O_3 = 100$) and TiO_2 (P-25; surface area, 50 m^2/g; anatase) were purchased and kindly provided by Tosoh Ltd. and Nippon Aerosil Ltd., respectively. Sulfamethazine (SMT, Aldrich), 4-amino-2, 6-dimethylpyrimidine (ADMP, 97%, Wako), and all other reagents, including acetonitrile, sulfuric acid, sodium hydroxide, and formic acid, were purchased and used without further purification.

Removal of SMT using RAOC

The RAOC reactor is shown in Fig. 1. The composite TiO_2–zeolite sheets were fixed on both sides of a stainless-steel disk with a diameter of 24 cm (ca. 900 cm^2 for both sides), and the disk was mounted in a laboratory-scale test tank, in which the bottom side was submerged in water. The proportion of the sheet area that was submerged in the water was approximately 45%. The preparation of the TiO_2–zeolite sheets was reported in our previous study (Fukahori et al. 2015). The sheets consist of TiO_2, zeolite, glass fiber, and alumina binder. The density of TiO_2 and zeolite in the sheet was 11.2 mg/cm^2, respectively (the ratio of TiO_2 and zeolite was 1: 1). SMT solution (2 L, 10 mg/L) was poured into the test tank and the disk was rotated slowly (10 rpm). The initial SMT concentration was set higher compared to that detected in natural environment or secondary effluent from wastewater treatment plant in order to clarify the degradation mechanism of SMT during RAOC treatment. For photocatalytic treatment, the top side of the disk exposed to air was irradiated with an ultraviolet lamp (FL287-BL365; Raytronics Corp.; maximum wavelength 365 nm) to overcome attenuation of the light intensity in water. The UV intensity at the surface of the composite sheet was measured using UV radiometer (UV-340C, CUSTOM) and set as 1 mW/cm^2 on average. The energy consumption during UV treatment was calculated from average UV intensity at the surface of the composite sheet, the sheet area that was irradiated with UV and UV irradiation time. The energy consumption for RAOC treatment was 1.782 kJ/h. The pH was adjusted to 7 using sulfuric acid or sodium hydroxide and measured by a portable pH meter (D-51; Horiba, Kyoto, Japan). RAOC treatment was conducted three times.

Quantitative analysis

After treatment, a sample aliquot was passed through a membrane filter (Dismic; pore size, 0.20 μm; Advantec, Ltd., Japan) prior to quantitative measurements. The SMT concentration in solution was measured using liquid chromatography tandem mass spectrometry (LC/MS/MS; Acquity UPLC-Xevo TQ; Waters, USA). The LC/MS/MS analysis was carried out using a BEH C18 column (2.1 × 150 mm; Waters) with a linear gradient from 10% acetonitrile (isocratic for 0.5 min) to 90% (0.5–7 min) in 0.05% formic acid at a

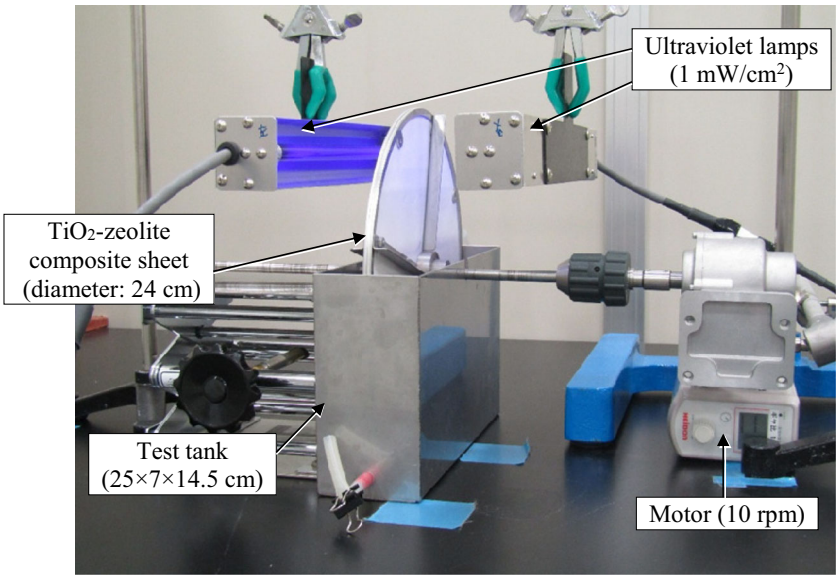

Fig. 1 The appearance of RAOC

constant flow rate of 0.3 mL/min. A photodiode array detector (PDA) was placed between the analytical column and the MS/MS, and the wavelength was set at 254 nm. To confirm the accuracy of the UPLC analysis, we measured the standard samples three times and the coefficient of variance of the peak area was confirmed to be < 5%. The structures of the intermediates were determined or deduced through comparison with standards or interpretation of the mass patterns obtained by LC/MS/MS.

The non-purgeable organic carbon (NPOC, mg-C/L) content in the treated water was measured using a Shimadzu TOC analyzer (TOC-5000A, Japan) based on CO_2 quantification by non-dispersive infrared analysis after high-temperature catalytic combustion. *NPOC* and $NPOC_0$ are the content of NPOC at time *t* and 0, respectively.

To measure the amount of SMT and NPOC content in the composite sheet, a piece of the composite sheet was cut and placed into 0.1 M sodium hydroxide solution. The solution was then sonicated for 1 min to elute SMT and organic compounds derived from intermediates from the sheet, and then the suspension was passed through a membrane filter. The SMT concentration and NPOC content in the supernatant were measured using LC/MS/MS and a TOC analyzer, and the amount of SMT and NPOC contained in the sheet was calculated.

The concentrations of NH_4^+, NO_3^-, and SO_4^{2-} in the treated water were measured using ion chromatography (DX-120; Dionex, Sunnyvale, CA, USA). The NH_4^+ concentration was measured using a CS12A column (4 × 250 mm; Dionex) with 19.8 mM methanesulfonic acid as the eluent (flow rate 1 mL/min). The NO_3^- and SO_4^{2-} concentrations were analyzed using an AS12A anionic column (4 × 200 mm; Dionex) and a mixture of 2.7 mM Na_2CO_3 and 0.3 mM $NaHCO_3$ (flow rate 1.5 mL/min).

Results and discussion

Removal of SMT using a RAOC reactor

Figure 2a shows the time courses of the amount of SMT in water and SMT adsorbed inside the composite sheet when an SMT solution was treated in the RAOC under dark conditions. After treatment for 6 h, 91.6% of SMT was removed from the water. Furthermore, the sum of the amount of SMT in the treated water and inside the sheet was unchanged if UV irradiation was not used. This result indicated that SMT was removed from water through adsorption, and the SMT adsorbed inside the composite sheet could be quantified by alkaline extraction. We have already revealed that there is no affinity between SMT and the component of the composite sheets such as P-25, the glass fiber, and the alumina binder (Fukahori et al. 2012, 2015); thus, the decrease of SMT concentration must be owing to adsorption on HSZ-385 inside the composite sheet. With respect to rate constant, Azizian reported on a new theoretical approach to adsorption rate kinetics and concluded that adsorption kinetics fit better to a pseudo-second-order model when the initial concentration of the solute is not high (Azizian 2004). In the present study, the initial concentration of the SMT was low (10 mg/L); therefore, a pseudo-second-order model was applied to the experimental data.

$$\frac{t}{q_t} = \frac{t}{q_e} + \frac{1}{k\,q_e^{\,2}} \tag{1}$$

where *k* (g/mol min) is the rate constant of the pseudo-second-order adsorption, and q_e (mol/g) and q_t (mol/g-zeolite) are the amount of SMT adsorbed on the zeolite at equilibrium and at *t* (min), respectively. The results are shown in Fig. 2a. The zeolite content in the composite sheet was 11.2 mg/cm^2, and

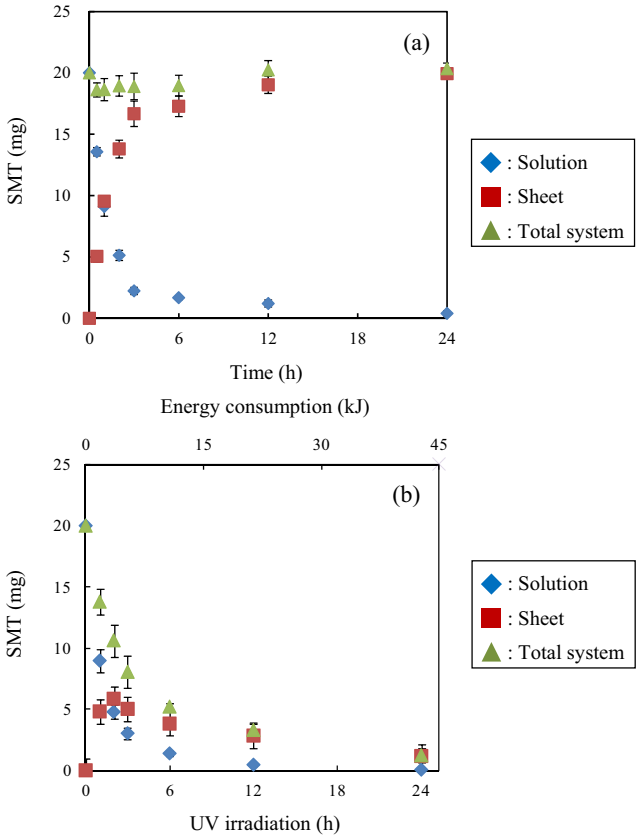

Fig. 2 Removal behavior of SMT using RAOC in solution (diamonds) and inside the sheet (squares) and in the total system (triangles) without (**a**) and with (**b**) UV irradiation. Error bars show standard deviations

900 cm^2 of composite was applied in the adsorption experiment; thus, approximately 10.1 g-zeolite was used for the treatment of 2 L of SMT solution. The value of k for RAOC was 1.77×10^3 g/mol min. The plot (t/q_t) versus t is shown in the supplementary material. The half-life time $t_{1/2}$, which is the time required to adsorb half the amount of q_e, is frequently used as a measure of the adsorption rate. The value of $t_{1/2}$ could be obtained by inserting $t = t_{1/2}$ and $q_t = q_e/2$ into Eq. (2):

$$t_{1/2} = \frac{1}{k\, q_e} \tag{2}$$

The value of $t_{1/2}$ for RAOC was 75 min. In our previous study, we evaluated the adsorption rate of SMT onto powder HSZ-385 and the value of $t_{1/2}$ at pH 4.7 was 3.53×10^5 g/mol min and 1.65×10^{-2} min, respectively (Fukahori et al. 2011). These results indicate that the adsorption rate of SMT by RAOC was substantially lower compared with that of zeolite powder. This occurred because TiO_2 and HSZ-385 particles were aggregated inside the sheet during the sheet-making process, causing low accessibility of the SMT molecules to the surfaces of TiO_2 and HSZ-385 in the composite sheet (Fukahori et al. 2003).

SMT in the aqueous phase decreased smoothly under UV irradiation and 90% of SMT was removed after 12 h of treatment (Fig. 2b). The amount of SMT adsorbed onto the sheet increased for 2 h owing to the adsorption of SMT onto zeolite inside the composite sheet, and then decreased. The amount of SMT inside the sheet was unchanged if UV irradiation was not used; therefore, SMT adsorbed inside the composite sheet was photocatalytically decomposed. As the disk was rotated, a part of the SMT solution was attached on the surface of the composite sheet and moved to the upper side of the disk, where it was irradiated with UV light and the SMT present in the solution on the surface was photocatalytically decomposed. Then, the SMT adsorbed onto the zeolite gradually desorbed into the water retained at the sheet surface because the adsorption of SMT onto zeolite inside the sheet was reversible. The desorbed SMT transferred to nearby TiO_2 surfaces, and further photodecomposition occurred within the composite sheets. Thus, the amount of SMT contained in the composite sheet decreased through the localized free movement of SMT inside the composite sheets.

At the initial stage, the SMT adsorption rate was presumably higher than the photocatalytic decomposition rate and, as a result, SMT accumulated inside the sheet. The amount of SMT inside the sheet gradually decreased after 2 h of treatment, indicating the adsorption sites of zeolite were regenerated and RAOC could remove SMT continuously. In addition to UV irradiation time, energy consumption is also shown in Fig. 2b. After 1 h of treatment, the amount of SMT remained in the total system was 13.8 mg; in other words, 6.2 mg of SMT was photocatalytically decomposed. The energy consumption for RAOC treatment was 1.782 kJ/h; therefore, required energy for SMT degradation was 0.29 kJ/mg-SMT. From the results of photocatalytic decomposition of SMT by TiO_2 powder (Fukahori et al. 2012), required energy for SMT degradation was 0.17 kJ/mg-SMT. Mentioned above, the adsorption rate constant of SMT for RAOC treatment was two orders lower than that for high-silica zeolite powder. Although the required energy for SMT degradation in RAOC treatment was slightly higher than that obtained using TiO_2 powder, negative effect of sheet formation for photocatalytic decomposition was quite little compared to that for adsorption. When TiO_2 powder is used for water treatment, the reaction efficiency tends to decrease with an increase of the reactor size because of light attenuation and scattering by water or TiO_2 powder itself (Wu et al. 2009; Bensaadi et al. 2014). In our RAOC reactor, the composite TiO_2–zeolite sheets are exposed to air and irradiated directly by UV light, which overcomes the problem of light attenuation.

Photocatalytic decomposition behavior of the intermediates

To investigate the photocatalytic decomposition behavior of SMT, we evaluated the NPOC content in the aqueous phase and inside the composite sheet and the formation and decomposition of intermediates. First, the time courses of NPOC content in the aqueous phase and inside the composite sheet during RAOC treatment were measured (Fig. 3a). The NPOC content derived from SMT (Fig. 3b) was calculated from the SMT concentration shown in Fig. 2b. In addition, NPOC content derived from intermediates was also calculated by subtracting the SMT-derived NPOC from the total NPOC content (Fig. 3c). In the aqueous phase, the total NPOC content quickly decreased and 60% of NPOC was removed after 3 h; however, the amount of NPOC was unchanged during treatment for 3–24 h. It has already been clarified that SMT was smoothly removed from the aqueous phase (Fig. 3b). However, the NPOC derived from intermediates in the aqueous phase increased and accumulated with treatment time (Fig. 3c). Therefore, the total NPOC content in the aqueous phase was unchanged during treatment for 3–24 h. Furthermore, the NPOC content inside the composite sheet indicated that the zeolite adsorbent contained in the sheet captures not only SMT but some intermediates, which were accumulated inside the sheet. At the initial stage, the NPOC content derived from intermediates inside the composite sheet increased and then decreased during treatment for 6–24 h. This behavior was similar to that of SMT inside the composite sheet. Conversely, the NPOC content derived from intermediates inside the aqueous phase gradually increased. The intermediates that could not be adsorbed onto the composite sheet may accumulate in the aqueous phase.

Next, the formation and decomposition behavior of the intermediates were evaluated using LC/MS/MS. The information about the molecular weight and structure of intermediates can be obtained by LC/MS/MS analysis. Abdelraheem et al. reported the decomposition of sunscreen ingredient PBSA by UV/H_2O_2 and revealed the degradation pathway of PBSA (Abdelraheem et al. 2016). In our previous study, SMT and some analogous compounds were treated by TiO_2 and the formation of seven intermediates formed with the photocatalytic decomposition of SMT, two types of monohydroxylated SMT, dihydroxylated SMT (SMT-2OH), hydroxylated sulfanilic acid (SA-OH), 4-amino-2, 6-dimethylpyrimidine (ADMP) and monohydroxylated ADMP (ADMP-OH), were confirmed and degradation pathway was also proposed (Fukahori and Fujiwara 2015). In addition, dihydroxylated ADMP (ADMP-2OH) was detected in this study and the behavior of six intermediates during the RAOC treatment was evaluated. The intermediates

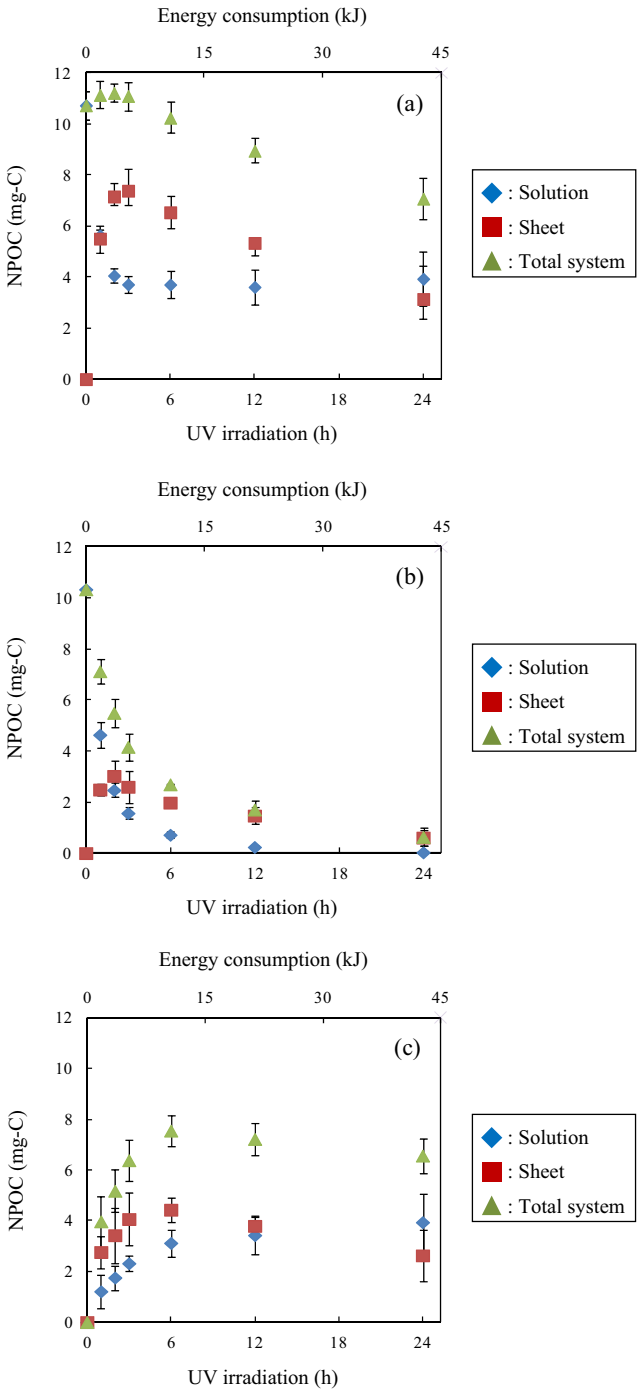

Fig. 3 Time courses of NPOC during RAOC treatment in solution (diamonds) and inside the sheet (squares) and in the total system (triangles). Total NPOC content (**a**). NPOC content derived from SMT (**b**) and intermediates (**c**). Error bars show standard deviations

contained in the aqueous phase and inside the sheet were analyzed by selective ion recording (SIR) mode of LC/MS/MS in a similar manner to the analysis of SMT. The proposed relationship between SMT and the six intermediates is shown in Fig. S1 in the supplementary material. The relative amounts of intermediates contained in the total system are expressed as a simple sum of the peak areas

of the intermediates detected in the aqueous phase and inside the sheet.

Figure 4 shows the time course of P_t/P_{max} of the intermediates observed during RAOC treatment of SMT, where P_t is the intermediate peak area in the aqueous phase, inside the sheet and in the total system, measured in SIR mode at treatment time t and P_{max} is the maximum peak area of each intermediate in the total system during the treatment. In other words, the relative amounts of the intermediates present in the aqueous phase, inside the composite sheet and in the total system, can be obtained from Fig. 4. In our previous work, we reported the formation of two types of monohydroxylated SMT intermediates; an aminophenyl moiety and a pyrimidinyl moiety were hydroxylated (abbreviated as Ph-OH and Pry-OH, respectively). These two intermediates formed at the initial treatment stage and reached a maximum amount after treatment for 3 h. After their formation, SMT-2OH, ADMP, ADMP-OH, and finally ADMP-2OH accumulated. This order

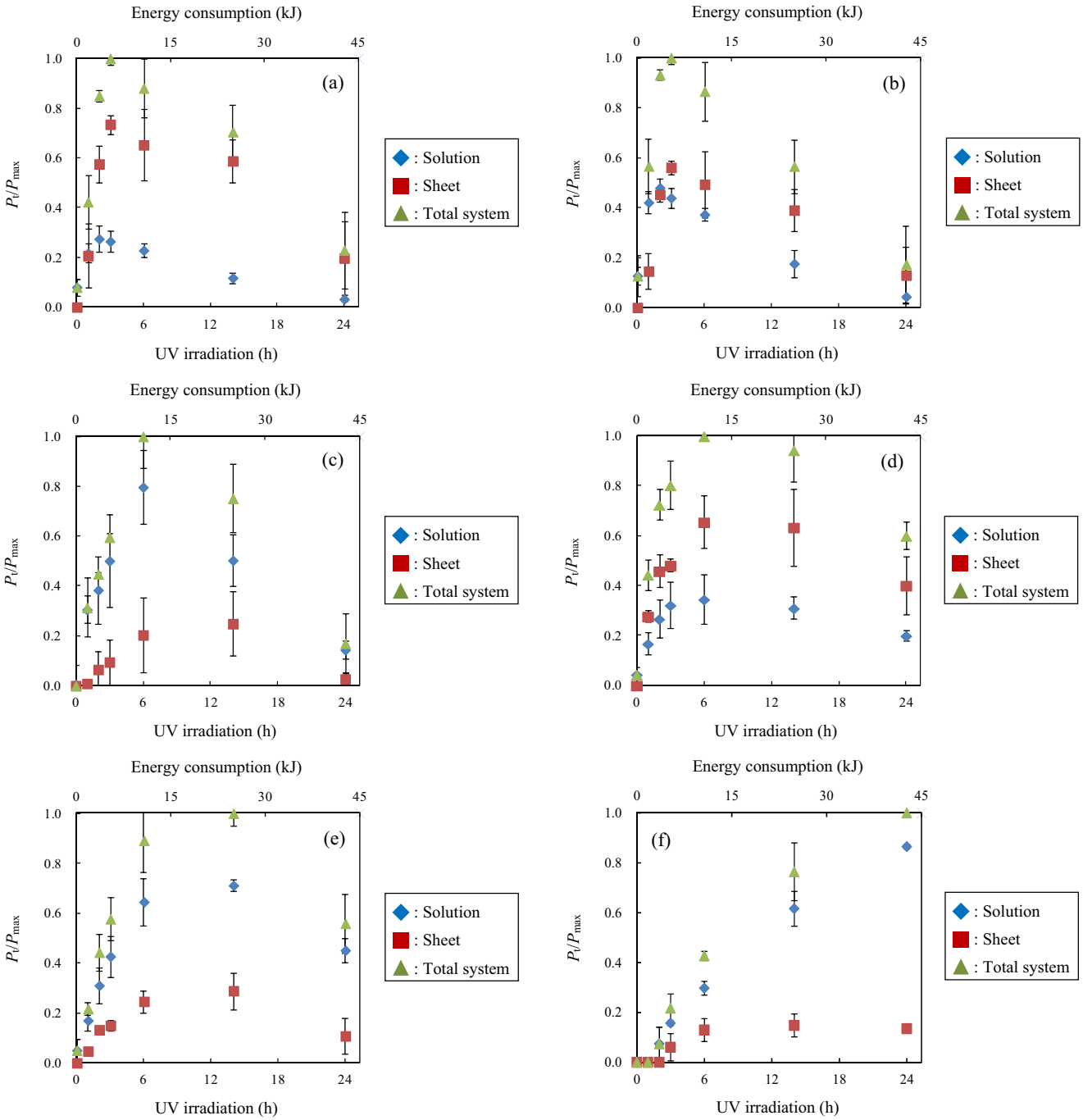

Fig. 4 Time courses of the ratios of major intermediates in solution (diamonds), inside the sheet (squares) and in the total system (triangles). **a** Ph-OH. **b** Pyr-OH. **c** SMT-2OH. **d** ADMP. **e** ADMP-OH. **f** ADMP-2OH. Error bars show standard deviations

is similar to that when TiO_2 powder was used (Fukahori and Fujiwara 2015). The proportion of Ph-OH in the aqueous phase and inside the composite sheet after treatment for 3 h was approximately 26 and 74%, indicating that a significant amount of Ph-OH was adsorbed inside the sheet (Fig. 4a). The adsorption mechanism of SMT onto HSZ-385 may be based on hydrophobic interactions (Fukahori et al. 2011). Ph-OH is more hydrophilic than SMT; however, the structure of Ph-OH is similar to SMT and it is easily adsorbed onto the zeolite and retained inside the sheet. Similar phenomena were confirmed for Pry-OH and ADMP (Fig. 4b, d); the proportions of Pry-OH or ADMP inside the composite sheet were lower than that of Ph-OH, presumably because they were slightly more hydrophilic than Ph-OH. Unlike monohydroxylated SMT, the percentage of SMT-2OH in the aqueous phase and inside the composite sheet after treatment for 6 h were approximately 80 and 20%, respectively (Fig. 4d). Similarly, the proportions of ADMP-OH and ADMP-2OH in the aqueous phase were higher than those inside the composite sheet (Fig. 4e, f). As they are more hydrophilic than monohydroxylated SMT and ADMP, low adsorption efficiency onto HSZ-385 was achieved and they could not be captured inside the composite sheet. These results corresponded to the behavior of NPOC content derived from intermediates, as shown in Fig. 3c.

Proposed degradation mechanism of SMT by RAOC

The time course of the inorganic ion concentrations during the RAOC treatment of SMT is depicted in Fig. 5. This confirmed the mineralization of SMT because nitrogen and sulfur atoms were converted to NH_4^+, NO_3^-, and SO_4^{2-} during the photocatalytic decomposition of organic compounds by TiO_2. Abdelraheem et al. also investigated the mineralization behaviors of organic compounds containing nitrogen and sulfur through UV/H_2O_2 system and clarified the formation rate of inorganic ions depended on the structure of parent compounds (Abdelraheem et al. 2015). The stoichiometric maximum inorganic nitrogen and sulfur concentrations expected were 2.01 mg-N/L and 1.15 mg-S/L after complete mineralization of SMT. The formation behavior of SO_4^{2-}, NH_4^+, and NO_3^- when a solution of SMT with a concentration of 10 mg/L was treated by TiO_2 powder was also reported in our previous study (Fukahori and Fujiwara 2015). We revealed that NH_4^+ formed through the dissociation of an amino group and cleavage of a sulfonamide group. NO_3^- was derived from two nitrogen atoms contained in the pyrimidine ring. SO_4^{2-} formed through cleavage of the sulfonamide group. The concentrations of NH_4^+ and SO_4^{2-} increased at the initial treatment stage, indicating that the amino and sulfanilmide groups were easily attacked and mineralized by photocatalysis. From these results, half of the nitrogen atoms seem to be converted to NH_4^+ and the other half to NO_3^-; therefore, the stoichiometric concentrations of NH_4^+ and NO_3^- obtained after complete mineralization were approximately 1.00 mg-N/L for both.

In this study, the NH_4^+ and SO_4^{2-} concentrations were 0.94 mg-N/L and 0.45 mg-S/L, respectively, after treatment by RAOC for 24 h, indicating that approximately 94% of the nitrogen derived from amino and sulfanilamide groups and 39% of the sulfur derived from sulfanilamide groups were mineralized. Almost no NO_3^- was detected, which indicated that the pyrimidinyl moiety of SMT was preserved and mineralization of the amino and sulfonamide groups proceeded preferentially. This result corresponded to the formation of ADMP, ADMP-OH, and ADMP-2OH. When SMT solution was treated by TiO_2 powder, the mineralization ratios of nitrogen derived from amino and sulfanilamide groups and sulfur were similar (Fukahori and Fujiwara 2015). Conversely, only 39% of sulfur was mineralized after treatment by RAOC for 24 h, indicating that the mineralization behavior of SMT treated by RAOC is different from that treated by TiO_2 powder. The SO_4^{2-} was formed through the cleavage of sulfonamide and the subsequent dissociation of a sulfonic group. The intermediate compounds with a sulfonic group, for example, hydroxylated sulfanilic acid, were detected in our previous study (Fukahori and Fujiwara 2015). Unfortunately, those intermediates were not detected during RAOC treatment. The intermediates with a sulfonic group are highly hydrophilic because sulfanilic acid had negative charge due to the dissociation of sulfonate group at pH 7. The adsorption of organic compounds onto high-silica zeolite is based on hydrophobic interaction; therefore, the intermediates with a sulfonic group are hardly adsorbed onto HSZ-385 inside the composite sheet. As an example, we used sulfanilic acid as a model compound to investigate the reaction mechanism of the TiO_2–zeolite composite and confirmed that no sulfanilic acid was adsorbed

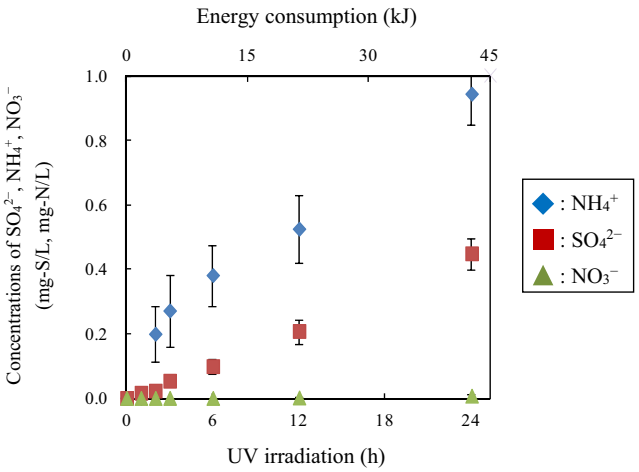

Fig. 5 Time course of inorganic ion concentrations formed through photocatalytic decomposition of SMT by RAOC; ammonium (diamonds), sulfate (squares), and nitrate (triangles). Error bars show standard deviations

onto HSZ-385 (Fukahori and Fujiwara 2014). The RAOC can be used to decompose compounds that can be adsorbed onto zeolite inside the sheet. Therefore, it was difficult to decompose intermediates containing a sulfonic group, resulting in low mineralization of sulfur. Furthermore, a part of ADMP, ADNP-OH, and ADMP-2OH, which form through the cleavage of the sulfonamide group, was adsorbed onto the composite sheet (Fig. 4d–f). These results strongly support nitrogen derived from sulfonamide group could be converted to NH_4^+ by RAOC treatment. Therefore, NH_4^+ reached its stoichiometric concentrations.

Conclusions

The removal of SMT and its intermediates from water using a RAOC equipped with TiO_2–high-silica zeolite composite sheets was investigated. SMT was removed from water through adsorption onto high-silica zeolite and subsequent photocatalysis by TiO_2 inside the composite sheet. Some hydrophobic intermediates such as hydroxylated SMT were also retained inside the composite sheet; on the other hand, hydrophilic intermediates were relatively distributed in water. Furthermore, the time courses of ion concentrations revealed the mineralization of nitrogen preferentially proceeded compared to sulfur and mineralization behavior of SMT treated by RAOC was different from that treated by TiO_2 powder. These results show that SMT and hydrophobic intermediates were captured by high-silica zeolite through hydrophobic interactions then photocatalytically decomposed, indicating RAOC was effective for the removal of both SMT and its intermediates.

Funding information This work was supported by the Core Research for Evolutional Science and Technology (CREST) program of the Japan Science and Technology Agency and JSPS KAKENHI Grant Number 16H02372. Papermaking was supported by the Ehime Institute of Industrial Technology Paper Technology Center.

References

Abdelraheem WHM, He X, Duan X, Dionysiou DD (2015) Degradation and mineralization of organic UV absorber compound 2-phenylbenzimidazole-5-sulfonic acid (PBSA) usingUV-254 nm/H_2O_2. J Hazard Mater 282:233–240

Abdelraheem WHM, He X, Komy ZR, Ismail NM, Dionysiou DD (2016) Revealing the mechanism, pathways and kinetics of UV_{254nm}/H_2O_2-based degradation of model active sunscreen ingredient PBSA. Chem Eng J 288:824–833

Azizian S (2004) Kinetic models of sorption: a theoretical analysis. J Colloid Interface Sci 276:47–52

Bensaadi Z, Yeddou-Mezenner N, Trari M, Medjene F (2014) Kinetic studies of β-blocker photodegradation on TiO_2. J Environ Chem Eng 2:1371–1377

Cao H, Lin X, Zhan H, Zhang H, Lin J (2013) Photocatalytic degradation kinetics and mechanism of phenobarbital in TiO_2 aqueous solution. Chemosphere 90:1514–1519

Dionysiou DD, Balasubramanian G, Suida MT, Khodadoust AP, Baudin I, Laîne JM (2000) Rotating disk photocatalytic reactor: development, characterization, and evaluation for the destruction of organic pollutants in water. Water Res 34(11):2927–2940

Fukahori S, Fujiwara T (2014) Modeling of sulfonamide antibiotic removal by TiO_2/high-silica zeolite HSZ-385 composite. J Hazard Mater 272:1–9

Fukahori S, Fujiwara T (2015) Photocatalytic decomposition behavior and reaction pathway of sulfamethazine antibiotic using TiO_2. J Environ Manag 157:103–110

Fukahori S, Ichiura H, Kitaoka T, Tanaka H (2003) Capturing of bisphenol A photodecomposition intermediates by composite TiO_2-zeolite sheets. Appl Catal B Environ 46:453–462

Fukahori S, Fujiwara T, Ito R, Funamizu N (2011) pH-dependent adsorption of sulfa drugs on high silica zeolite: modeling and kinetic study. Desalination 275:237–242

Fukahori S, Fujiwara T, Ito R, Funamizu N (2012) Photocatalytic decomposition of crotamiton over aqueous TiO_2 suspensions: determination of intermediates and the reaction pathway. Chemosphere 89(3): 213–220

Fukahori S, Fujiwara T, Funamizu N, Matsukawa K, Ito R (2013) Adsorptive removal of sulfonamide antibiotics in the livestock urine using high-silica zeolite. Water Sci Technol 67(2):319–325

Fukahori S, Fujiwara T, Ito R, Funamizu N (2015) Sulfonamide antibiotic removal and nitrogen recovery from synthetic urine by the combination of rotating advanced oxidation contactor and methylene urea synthesis process. Water Sci Technol 72(2):238–244

Gao S, Zhao Z, Xu Y, Tian J, Qi H, Lin W, Cui F (2014) Oxidation of sulfamethoxazole (SMX) by chlorine, ozone and permanganate—a comparative study. J Hazard Mater 274:258–269

Hegedűs P, Szabó-Bárdos E, Horváth O, Szabó P, Horváth K (2017) Investigation of a TiO_2 photocatalyst immobilized with poly(vinylalcohol). Catal Today 284:179–186

Ito M, Fukahori S, Fujiwara T (2014) Adsorptive removal and photocatalytic decomposition of sulfamethazine in secondary effluent using TiO_2-zeolite composites. Environ Sci Pollut Res 21:834–842

Ji Y, Ferronato C, Salvador A, Yang X, Chovelon JM (2014) Degradation of ciprofloxacin and sulfamethoxazole by ferrous-activated persulfate: implications for remediation of groundwater contaminated by antibiotics. Sci Total Environ 472:800–808

Kim H, Hong Y, Park J, Sharma VK, Cho S (2013) Sulfonamides and tetracyclines in livestock wastewater. Chemosphere 91:888–894

Kordkandi SA, Motlagh MA (2018) Optimization of peroxone reaction rate using metaheuristic approach in the dearomatization and discoloration process. Environ Prog Sustain Energy 37(2):695–702

Kordkandi SA, Rasoul A (2015) Modeling and kinetics study of acid anthraquinone oxidation using ozone: energy consumption analysis. Clean Techn Environ Policy 17(8):2431–2439

Lapworth DJ, Baran N, Stuart ME, Ward RS (2012) Emerging organic contaminants in groundwater: a review of sources, fate and occurrence. Environ Pollut 163:287–303

Li W, Shi Y, Gao L, Liu J, Cai Y (2013) Occurrence and removal of antibiotics in a municipal wastewater reclamation plant in Beijing, China. Chemosphere 92:435–444

Lian J, Qiang Z, Li M, Bolton JR, Qu J (2015) UV photolysis kinetics of sulfonamides in aqueous solution based on optimized fluence quantification. Water Res 75:43–50

Prieto-Rodriguez L, Miralles-Cuevas S, Oller I, Agüera A, Puma G, Malato S (2012) Treatment of emerging contaminants in wastewater treatment plants (WWTP) effluents by solar photocatalysis using low TiO_2 concentrations. J Hazard Mater 211-212:131–137

Rimoldi L, Meroni D, Cappelletti G, Ardizzone S (2017) Green and low cost tetracycline degradation processes by nanometricand immobilized TiO_2 systems. Catal Today 281:38–44

Wu RJ, Chen CC, Chen MH, Lu CS (2009) Titanium dioxide-mediated heterogeneous photocatalytic degradation of terbufos: parameter study and reaction pathways. J Hazard Mater 162:945–953

Yap PS, Lim TT (2012) Solar regeneration of powdered activated carbon impregnated with visible-light responsive photocatalyst: factors affecting performances and predictive model. Water Res 46:3054–3064

Yap PS, Cheah YL, Srinivasan M, Lim TT (2012) Bimodal N-doped P25-TiO_2/AC composite: preparation, characterization, physical stability, and synergistic adsorptive-solar photocatalytic removal of sulfamethazine. Appl Catal A Gen 427–428:125–136

Zhang L, Anderson WA, Zhang Z (2006) Development and modeling of a rotating disc photocatalytic reactor for wastewater treatment. Chem Eng J 121:125–134

Zhao C, Deng H, Li Y, Liu Z (2010) Photodegradation of oxytetracycline in aqueous by 5A and 13X loaded with TiO_2 under UV irradiation. J Hazard Mater 176:884–892